PROCEEDINGS OF SPIE

SPIEDigitalLibrary.org/conference-proceedings-of-spie

ZnO for solar cell and thermoelectric applications

Chuanle Zhou, Amirhossein Ghods, Kelcy L. Yunghans, Vishal G. Saravade, Paresh V. Patel, et al.

SPIE.

Invited Paper

ZnO for Solar Cell and Thermoelectric Applications

Chuanle Zhou[a], Amirhossein Ghods[a], Kelcy L. Yunghans[a], Vishal G. Saravade[a], Paresh V. Patel[a], Xiaodong Jiang[b], Bahadir Kucukgok[b], Na Lu[b], and Ian Ferguson[a,*]

[a]Engineering and Computing, Missouri University of Science and Technology, Rolla MO 65409
[b]Lyles School of Civil Engineering, School of Materials Engineering, Birck Nanotechnology Center, Purdue University, West Lafayette, IN 47907, USA

ABSTRACT

ZnO-based materials show promise in energy harvesting applications, such as piezoelectric, photovoltaic and thermoelectric. In this work, ZnO-based vertical Schottky barrier solar cells were fabricated by MOCVD deposition of ZnO thin films on ITO back ohmic contact, while Ag served as the top Schottky contact. Various rapid thermal annealing conditions were studied to modify the carrier density and crystal quality. Greater than 200 nm thick ZnO films formed polycrystalline crystal structure, and were used to demonstrate Schottky solar cells. I-V characterizations of the devices showed photovoltaic performance, but but need further development. This is the first demonstration of vertical Schottky barrier solar cell based on wide bandgap ZnO film.

Thin film and bulk ZnO grown by MOCVD or melt growth were also investigated in regards to their room-temperature thermoelectric properties. The Seebeck coefficient of bulk ZnO was found to be much larger than that of thin film ZnO at room temperature due to the higher crystal quality in bulk materials. The Seebeck coefficients decrease while the carrier concentration increases due to the crystal defects caused by the charge carriers. The co-doped bulk $Zn_{0.96}Ga_{0.02}Al_{0.02}O$ showed enhanced power factors, lower thermal conductivities and promising ZT values in the whole temperature range (300-1300 K).

Keywords: ZnO, wide bandgap, solar cell, thermoelectric

1. INTRODUCTION

Zinc Oxide (ZnO), as a semiconductor with wide and direct bandgap, greater than 90% transparency in visible region, high electron mobility, and thermal conductivity, has been investigated in different electronic applications.[1–15] Short-wavelength ultraviolet (UV) region photodetectors use ZnO especially due to its wide bandgap and large exciton binding energy (60 meV).[7] As an UV LED material, ZnO is superior over nitrides in thermal stability and also in resistance to chemical reaction and oxidation.[8] Transition metal-doped ZnO (TMD) has also attracted interests in regard to existence of room temperature ferromagnetism.[9]

ZnO has recently been intensively investigated as a candidate material for sustainable energy applications. ZnO is used in piezoelectric devices instead of piezoelectric (Pb, Zr)TiO_3 (PZT) due to its minimal effect on the enviorment.[16] ZnO nanowires or nanorods have been developed into piezoelectric generators which can be used as transparent, flexible self-powered pressure sensors or generators.[17–20] ZnO is used as the active layer to create p-n or n-n hetero-junction and also as antireflection coating in hetero-junction solar cells.[6] ZnO has the potential to replace TiO_2 in dye sensitized solar cells (DSSC) due to its higher electron mobility and similar conduction band energy level.[5] Compared to the conventional thermoelectric (TE) materials such as Bi_2Te_3-, PbTe- and SiGe-based alloys that have high toxicity, low abundance, and poor chemical stability at high temperature, ZnO-based materials are more attractive for TE applications as they are environmental friendly, cost-effective and thermally stable at high temperatures. Therefore, ZnO-based materials recently become interesting for their promising TE properties in wide temperature range (300 K-1300 K).[10–15] The current paper will represent recent studies on ZnO-based vertical Schottky barrier solar cells as a first demonstration of such solar cell structures, and thermoelectric properties of bulk and thin film ZnO for high temperature thermoelectric applications.

*Further author information: (Send correspondence to Ian Ferguson)
E-mail: ianf@mst.edu

Oxide-based Materials and Devices VIII, edited by Ferechteh H. Teherani, David C. Look, David J. Rogers, Ivan Bozovic. Proc. of SPIE Vol. 10105, 101051K · © 2017 SPIE
CCC code: 0277-786X/17/$18 · doi: 10.1117/12.2262772

2. SCHOTTKY BARRIER SOLAR CELL

2.1 Introduction

Single-junction narrow bandgap solar cells, e.g. Si-, CIGS-, CdTe-based solar cells, are dominating the current solar cell market,[21] although their efficiency is limited[22] to less than 25%. For the next generation solar cells based on nanostructured materials, wide bandgap material are necessary for sufficient harvesting from the solar spectrum to achieve higher power conversion efficiency.[21,23] The main problem with wide bandgap cells is the required doping, especially p-type doping, which produces vacancies and a host of crystal defects that function as recombinant traps. These traps result in low short circuit currents and low efficiencies. In many wide bandgap materials, including most II-VI semiconductors, it is very difficult to fabricate satisfactory junctions, and highly doped p+ layers for tunnel junctions or metallization contacts. Schottky barrier solar cells can be a substitute structure for wide bandgap devices because of their simplicity, low cost and lack of p-doped layers.

ZnO-based Schottky diode has been used as ultraviolet (UV) photodetectors, where the devices are in metal-semiconductor-metal (MSM) lateral structure.[24–28] ZnO nanorod arrays have also formed Schottky barrier solar cells.[29,30] The current work is the first to study vertical Schottky solar cells based on ZnO thin film. ZnO thin films were grown by Metal Organic Chemical Vapor Phase Deposition (MOCVD) under optimized growth process. The crystal quality and electrical property of ZnO films with various thickness and rapid thermal annealing (RTA) conditions were studied. A ZnO-based vertical Schottky solar cell was fabricated using indium tin oxide (ITO) as the back ohmic contact and Ag as the front Schottky contact. The I-V performance was characterized to demonstrate the device photovoltaic performance.

2.2 Fabrication

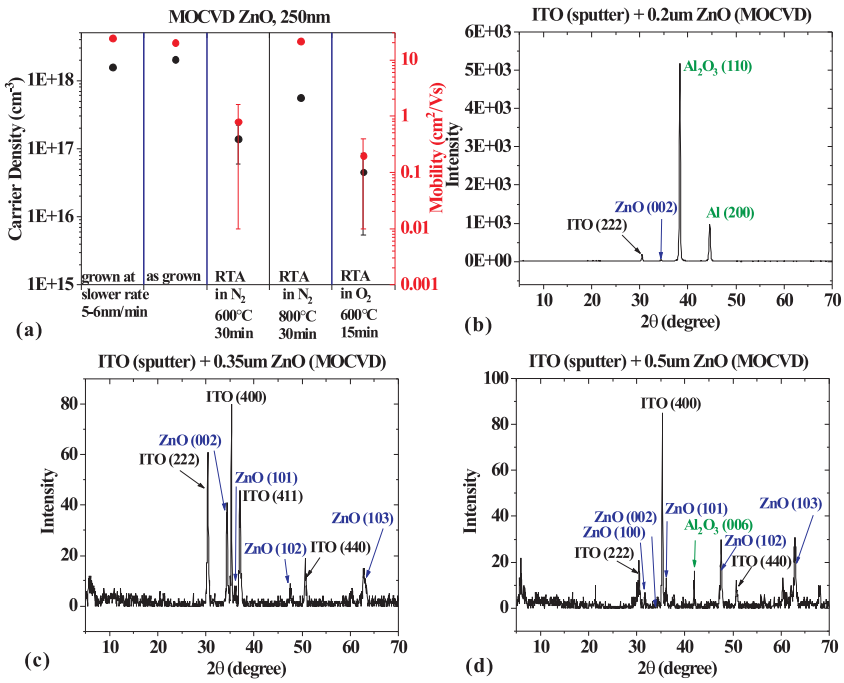

Figure 1. (a)Hall measurement of ZnO films grown by MOCVD on sapphire substrate. XRD measurement of MOCVD grown ZnO films with the thicknesses (b) 200 nm (c) 350 nm (d) 500 nm

ZnO thin films were deposited by MOCVD, which used O_2 as the oxygen source, diethyl zinc (DEZn) as the Zn source and N_2 as carrier gas. The growth rate is affected by adsorption of reactants onto the surface and cracking efficiency of precursors, which can be adjusted by the disk rotation speed and growth pressure. The crystal quality depends on the gas flow configurations, substrate temperature and heat distribution. The

MOCVD growth condition was optimized to be substrate temperature at 550^{o}C, disk rotation speed at 800 rpm, growth pressure at ∼5 torr, DEZn flow rate at 100 SCCM, O_2 flow rate at 1000 SCCM, and bubbler pressure at 146 torr. Compared to sputtered ZnO films, the MOCVD grown ZnO films shows much higher peaks in photoluminescence (PL) and X-ray powder diffraction (XRD) measurement, which demonstrates better crystal quality. ZnO grown on sapphire substrate showed better quality than those grown on n-Si substrate, due to the similar hexagonal crystal structure of ZnO and sapphire while different from the cubic structure of Si. The as grown ZnO films have an electron density of $\sim 3\times10^{18}$ /cm^3 and an electron mobility of ∼25 cm^2/Vs.

The ZnO films were annealed in different rapid thermal process (RTP) to modify the carrier density, and improve the crystal quality. Various annealing conditions includes N_2, O_2 or 80% N_2 + 20% O_2 gas environment, 400^{o}C, 600^{o}C or 800^{o}C substrate temperatures, and 15 min or 30 min duration. The annealing had reduced electron densities and mobilities 1-2 orders compared to the as grown ZnO films (Fig. 1(a)). Similar reduction of electron densities and mobilities after heat treatment was resulted from the reduction of oxygen vacancy and further defect creation.[31–33] Annealing in O_2 incorporated oxygen into the grains and the grain boundaries, and thus reduced the electron density more than that from the N_2 environment. Annealing with longer duration and at higher substrate temperature can lead to the grain growth, so the electron mobility was higher than those annealed at lower temperature.

The ZnO-based solar cells were fabricated by using an ITO layer as the back ohmic contact, which was first sputtered on sapphire (002) substrate at 300 ^{o}C for 45 min, resulting in a thickness of ∼210 nm. ZnO thin films were then grown on ITO layers by MOCVD of the thickness varying from 200 nm to 500 nm. The XRD characterization of the ZnO films on ITO with different thicknesses (Fig.1(b-d)) showed that 200 nm ZnO film on ITO has very weak peak for ZnO crystal, while thicker ZnO films with 350 nm and 500 nm thicknesses showed multiple ZnO crystal peaks. The 200 nm ZnO film on ITO may have amorphous or powder structure, while thicker ZnO films on ITO relax to form polycrystal structure. Similar polycrystalline structured silicon has been developed in solar-grade over large areas and applied in the commercial solar cell market.[23,34]

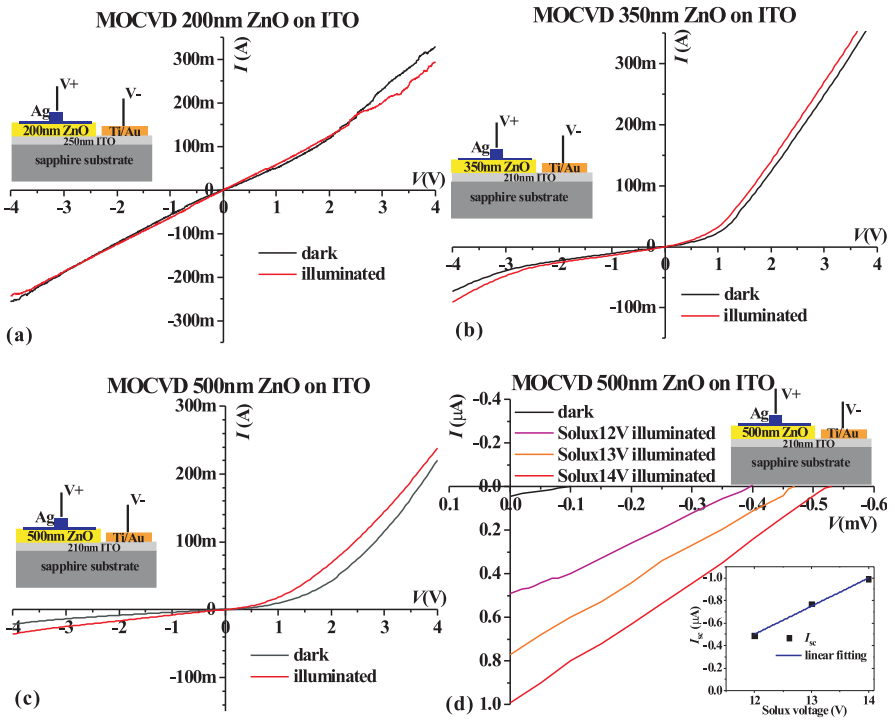

Figure 2. I-V characterization of ZnO-based vertical solar cells (a) 200 nm ZnO on ITO (b) 350 nm ZnO on ITO (c) 500 nm ZnO on ITO (d) V_{OC} and I_{SC} measurement of 500 nm ZnO-based solar cell under various illumination intensities

Since the thin films were deposited on the whole wafer, the ohmic contact pattern was etched down from ZnO surface to the ITO layer using HCl solution, followed by Ti/Au (20/80 nm) deposition as a highly conducting metal pad on ITO for probing. After H_2O_2 treatment, a 10 nm semi-transparent Ag was deposited on ZnO as the Schottky contact, followed by a 100 nm Ag Schottky contact pad on part of the 10nm Ag Schottky contact for measurement. The I-V measurement proved that ITO created ohmic contact on ZnO films. Ti/Au ohmic contact on ITO was characterized by transmission line measurement (TLM) to be 2.5×10^{-4} Ω/cm^2.

2.3 Characterization and Discussion

The ZnO-based solar cells were characterized using Keithley 4200 for the I-V performance in dark or solar simulator illumination (Fig. 2). Ag is typically used as Schottky contact for n-ZnO epi layers.[24,25,35,36] However, the 200 nm ZnO-based Ag-ZnO-ITO structure showed linear instead of rectified I-V curve (Fig. 2(a)), demonstrating that the Ag-ZnO junction is ohmic instead of Schottky. The previous XRD already showed the 200 nm ZnO film with amorphous or powder crystal structure, so the electrical band structure and the Ag-ZnO-ITO band alignment was not as the same as the bulk ZnO condition.

Thicker ZnO-based Ag-ZnO-ITO structure, such as 350 nm and 500 nm ZnO, showed rectified I-V curves (Fig. 2(b,c)), demonstrating Schottky-like Ag-ZnO. The threshold voltage is 1-1.2 V. The I-V curves were fitted in the diode current equation:

$$I = I_s[exp(\frac{q(V-IR)}{nk_BT}) - 1], \tag{1}$$

where I_s is the reverse saturation current, V is the applied voltage and R is the series resistance. The ideality factor n were greater than 10 for both 350 nm and 500 nm ZnO-based solar cells. Similar anomalously high ideality factors ($n = 3-5$) in n-ZnO-based Schottky diodes were observed before,[37,38] which could be attributed to an additional charge layer at the Schottky contact accounting for the ionized defects in the depletion region. The short circuit current I_{SC} and open circuit voltage V_{OC} of 350 nm and 500 nm ZnO-based vertical Schottky solar cells were calibrated under various illumination intensities (Fig. 2(d)). The short circuit currents I_{SC} showed linear increase with the increased illumination intensity from Solux broadband light bulb (inset of Fig. 2(d)), demonstrating the photovoltaic response. However, the short circuit currents I_{SC} were in the order of 0.1 μA and the open circuit voltages V_{OC} were in the order of 0.1 mV. These low I_{SC}, V_{OC} and non-ideal I-V curves may due to the polycrystalline structure of the thick ZnO films (measured by XRD, Fig. 1(c,d)), where the majority carrier traps around the grain boundaries resulting in depletion zones bend the energy band[31] and changed the band alignment between ZnO and Ag.

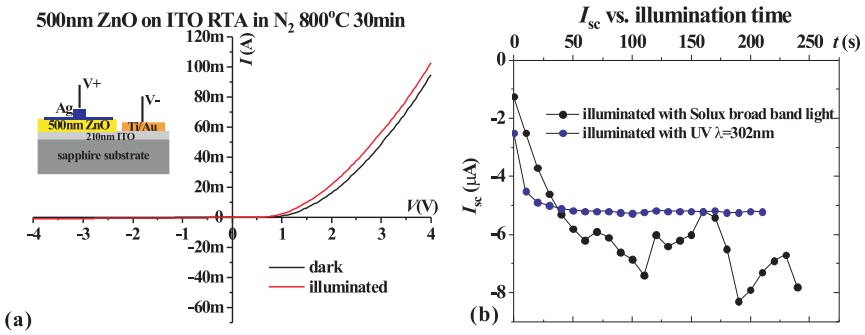

Figure 3. I-V characterization of RTP ZnO-based vertical solar cells (a) I-V (b) time dependent I_{SC}

The annealed ZnO-based solar cells were also fabricated and characterized. These devices had a threshold voltage of 1.5 V (Fig. 3(a)) and an ideality factor of 13.8. The annealed ZnO film had lower electron density and mobility than the as-grown ZnO film, and thus higher series resistance, lower short circuit current I_{SC} and lower open circuit voltage V_{OC}. The short circuit current I_{SC} was not stable after illumination (Fig. 3(b)), showing deep trap for electrons in the bandgap caused by growing defects after heat treatment.

3. THERMOELECTRICAL PROPERTIES

3.1 Introduction

TE materials and devices have attracted much attention for their ability to directly convert waste heat from cars, power plants and aircrafts into electrical power.[39,40] TE materials and devices have shown promising results; however, their applications are limited due to their low TE conversion efficiencies.[41,42] The TE conversion efficiency is determined by the dimensionless figure-of-merit ZT, which is defined as:

$$ZT = \frac{S^2 \sigma T}{\kappa_l + \kappa_e}, \tag{2}$$

where S is the Seebeck coefficient, σ is the electrical conductivity, T is the absolute temperature, κ_e is the electronic thermal conductivity and κ_l is the lattice thermal conductivity.[43] Large value of ZT is required to achieve high-performance TE materials and devices. However, κ_e and the power factor ($PF = S^2\sigma$) are interdependent parameters via Wiedemann-Franz function,[44] which is preventing to obtain high ZT values.[45,46] Therefore, more efforts have been devoted to reduce the κ_l. For example, alloying and nanostructuring TE materials increase the phonon scattering at boundaries and interfaces,[47] which can decrease the lattice κ_l without degrading the σ too much.

Doping group III elements (Al, Ga, In) has been utilized as the very efficient method to improve the TE properties of ZnO by decreasing the κ_l and enhancing the σ simultaneously.[48] For instance, aluminum-doped bulk ZnO alloy ($Zn_{0.98}Al_{0.02}O$) and indium-doped ZnO alloy[13] were reported to have ZT values of 0.30 at 1273 K and 0.45 at 1000 K,[49] respectively. Furthermore, TE properties have been recently improved by co-doping ZnO with Al and Ga, and ZT values of 0.47 at 1000 K and 0.65 at 1273 K with Al and Ga concentrations of 2% have been achieved, respectively.[14] Up to our knowledge, these are the highest ZT values reported for n-type ZnO based bulk materials.

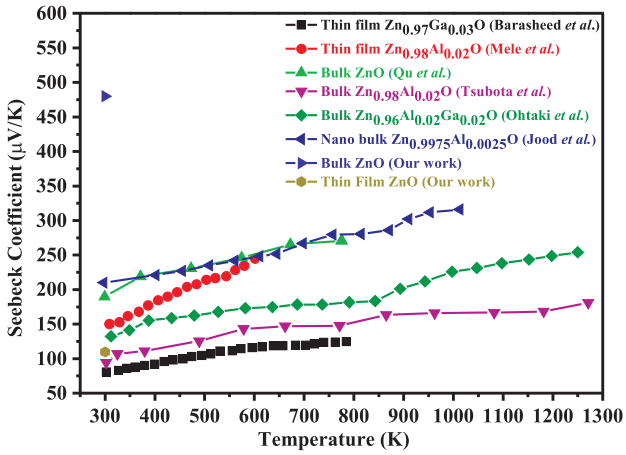

Figure 4. Temperature dependence of the absolute Seebeck coefficient between 300 K and 1300 K for ZnO-based TE materials

This work measured the room-temperature Seebeck coefficient and power factor (PF) of thin film and bulk ZnO grown by MOCVD and melt growth, respectively. The temperature dependence and carrier concentration dependence of the Seebeck coefficients and PF of both thin film ZnO and bulk ZnO were studied. The temperature-dependent TE properties of ZnO-based alloys were also reviewed.

3.2 Experiment

The thin film ZnO samples were grown on sapphire substrate along c-axis by MOCVD. The bulk ZnO samples were provided by Cermet Inc using melt growth method. The standard in-plane Seebeck measurement was

performed by using the integral method. More details about the experimental setup and the theory were reported elsewhere.[50] The in-plane electrical conductivities of both bulk ZnO and thin film ZnO were characterized by Van der Pauw hall measurement using Ecopia HMS-3000 Hall Measurement System. The metal ohmic contact (Ti/Al/Ti/Au) was deposited on the top of the sample surface as the electric electrodes by using e-beam evaporation.

3.3 Results and Discussion

Fig. 4 shows the temperature dependence of the absolute S values of ZnO-based TE materials from 300 K to 1300 K. It is observed that the absolute S values of all ZnO-based materials increase with the temperature rising because of the stronger lattice scattering at higher temperature regime. The absolute S values are greatly enhanced for the bulk ZnO and nano-bulk Al-doped ZnO samples due to the less disordered crystal structure or less stress existing in their crystals. For Ga-doped ZnO alloys, the bulk ZnO co-doped with Al and Ga has larger S value[14] than that of thin film[10] $Zn_{0.97}Ga_{0.03}O$ in the temperature range (300-800 K). In terms of the ZnO-based alloys doped with Al, the S value of the nano bulk ZnO with 0.25% Al-doping exhibits higher S value than those of the thin film $Zn_{0.98}Al_{0.02}O$ and the bulk[11,13,15] $Zn_{0.98}Al_{0.02}O$ from 300 K to 600 K. The reason for this could be the less 0.25% Al-doping in the nano bulk ZnO samples causes less defects in its crystal compared to those 2% Al-doping ZnO-based alloys. The difference between our data and reported S value for the bulk ZnO[12] at 300 K could be caused by the different growth methods since the S value can be largely affected by the defects density related to growth methods. Our data shows the S of bulk ZnO is much higher than that of thin film ZnO grown by MOCVD. This might be due to the fact that the bulk ZnO has higher crystal quality than the thin film ZnO.

The carrier concentration dependent S of the bulk ZnO and the thin film ZnO grown was investigated at room temperature. For the bulk ZnO, the S decreased from 772 μV/K to 405 μV/K with the carrier concentration increasing from 1.35×10^{16} to 2.01×10^{17} cm^{-3}. The S of thin film ZnO reduced from 113 μV/K to 10 μV/K as the carrier concentration increases from 3.31×10^{17} to 1×10^{20} cm^{-3}. The reason is that higher carrier density can result in more defects in the crystal due to the much more charge carriers.

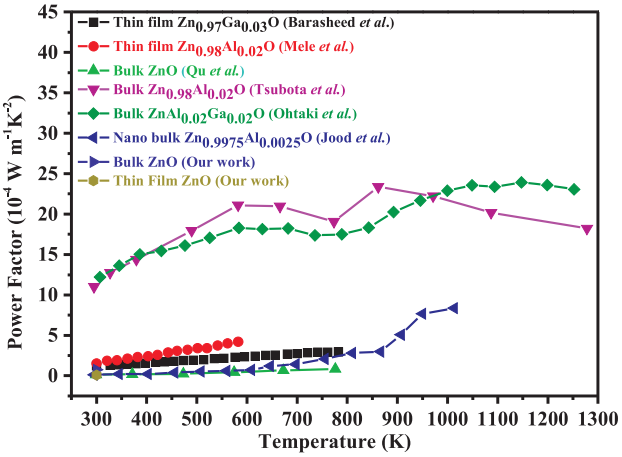

Figure 5. Temperature dependence of the power factor ($PF = S^2\sigma$) between 300 K and 1300 K for ZnO-based TE materials

Fig. 5 exhibits the temperature-dependent PF of ZnO-based TE materials, and it can be seen that PF value increases with temperature. Although the S values are very large for the Al-doped nano-bulk ZnO and bulk ZnO samples as shown in Fig. 4, the electrical conductivities of these samples are seriously degraded, hence their PF values are very small(Fig. 5). The bulk $Zn_{0.96}Al_{0.02}Ga_{0.02}O$ and $Zn_{0.98}Al_{0.02}O$ alloys indicate higher PF values than other ZnO-based materials in the temperature range from 300 K to 1300 K.[13,14] This might be attributed to the less stress existing in the bulk materials and higher electrical conductivities. Because the

doped Al^{3+} and Ga^{3+} usually substitute for Zn^{2+} in ZnO and act as n-type donors, which can highly enhance the electrical property of ZnO. Furthermore, the largest PF value (23.9×10^{-4} W/mK^2) was obtained in bulk $Zn_{0.96}Al_{0.02}Ga_{0.02}O$ at 1147 K.[13] At 300 K, our PF values of thin film ZnO and bulk ZnO can be comparable with those of thin film $Zn_{0.98}Al_{0.02}O$ and thin film $Zn_{0.97}Ga_{0.03}O$.[10,11]

Fig. 6 reveals the temperature-dependent thermal conductivities (κ) and ZT values of the bulk ZnO, the bulk $Zn_{0.98}Al_{0.02}O$ and $Zn_{0.96}Al_{0.02}Ga_{0.02}O$ samples.[12–14] The κ is dominated by κ_l in ZnO-based alloys due to their low electrical conductivity. It is known that the simple crystal structure can make the thermal conduction more efficient because of lattice (phonon) vibrations. Generally, the crystal structure will become more disordered or relatively complex with the increasing temperature or alloying. Therefore, the thermal conductivities of these ZnO-based TE materials decrease with the increasing temperature from 300 K to 1300 K and Al (Ga) doping concentration (0%-2%) (Fig. 6(a)). The dually doped $Zn_{0.96}Al_{0.02}Ga_{0.02}O$ sample shows the lowest κ of 5 W/mK at 1027 K compared to other two ZnO-based alloys. Additionally, among the ZnO-based TE materials, $Zn_{0.96}Al_{0.02}Ga_{0.02}O$ sample has the highest ZT values of 0.47 at 1000 K and 0.65 at 1247 K. Because co-doping ZnO with Al and Ga can increase the Al solubility limit in ZnO, which yields higher electrical conductivity. In the meanwhile, once more Al is doped into ZnO, the κ can be largely reduced due to the increased alloy scattering of phonons.

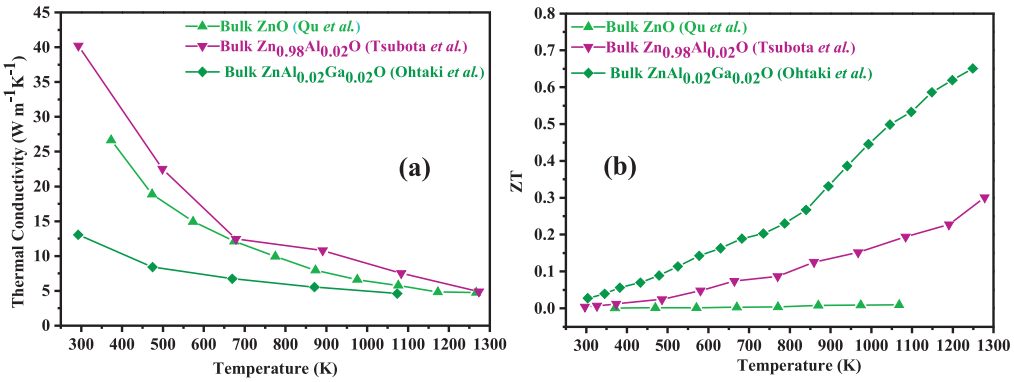

Figure 6. The temperature dependence of (a) the thermal conductivity and (b) ZT of ZnO-based TE materials

4. CONCLUSION

In conclusion, ZnO-based vertical Schottky solar cells was fabricated using ZnO thin film, ITO back ohmic contact and Ag front Schottky contact. The MOCVD deposited ZnO film has amorphous or power crystal structure under 200 nm and polycrystalline structure in the thicker films. The thick ZnO films showed Schottky rectified I-V curve for Ag-ZnO structure, but the polycrystalline structure changed the band alignment of Ag-ZnO junction and degraded the performance of the solar cell. The short circuit current I_{SC} and open circuit voltage V_{OC} were in the order of 0.1 μA and 0.1 mV, respectively, and both I_{SC} and V_{OC} increased with increasing illumination, demonstrating the photovoltaic performance of the device. Various RTP conditions on the ZnO films were studied, where the annealed ZnO films had lower electron density and mobility, and the unstable I_{SC} of the annealed ZnO-based solar cells showed deep traps in the bandgap which caused by heat treatment. This is the first demonstration for wide bandgap ZnO-film-based vertical Schottky solar cell.

In addition to the photovoltaic application, the TE properties of bulk ZnO and thin film ZnO grown by MOCVD were also studied at room temperature. It was observed that the Seebeck coefficient of bulk ZnO is much larger than that of thin film ZnO at room temperature. With the carrier concentration increasing, the Seebeck coefficients of both thin film ZnO and bulk ZnO decrease as the more charge carriers create more defects in the crystal. According to the literature review on the high-temperature TE properties of ZnO-based materials, the 0.25% atom Al-doping nano-bulk ZnO and bulk ZnO show very good Seebeck coefficients from 300 K to 800 K while the co-doped bulk $Zn_{0.96}Ga_{0.02}AlO$ reveal higher power factor value, lower thermal conductivity and the largest ZT value in the temperature range (300 K to 1300 K). Therefore, creating controlled defect

structures in ZnO crystal by doping group III elements (Al, Ga) can decouple phonon and electron transport, further improving the thermoelectric properties of ZnO based materials.

The results obtained in this work demonstrate ZnO as a candidate material for sustainable and renewable energy applications. As a material that has recently become interesting in solar cell and thermoelectric applications, ZnO thin films still need improvement in the sense of material quality, and optical and thermoelectric properties.

ACKNOWLEDGMENTS

The work on thermoelectric properties of ZnO was supported by NSF CAREER support (CMMI- 1560834).

REFERENCES

[1] A.Janotti and de Walle, C., "Free-space optical wavelength diversity scheme for fog migration in a ground-to-unmanned-aerial-vehicle communications link," *Opt. Eng.* **45**, 086001 (2006).

[2] Z.R.Khan, M.S.Khan, M.Zulfequar, and M.S.Khan, "Optical and structural properties of zno thin films fabricated by sol-gel method," *Mater. Sci. Appl.* **2**, 340 (2011).

[3] X.Ma, P.Chen, R.Zhang, and D.Yang, "Optical properties of sputtered hexagonal cdzno films with bandgap energies from 1.8 to 3.3 ev," *J. Alloys and Comp.* **509**, 6599 (2011).

[4] Ting, M., Reis, R., Jaquez, M., O.D.Dubon, Mao, S., Yu, K., and Walukiewicz, W., "Electronic band structure of zno-rich highly mismatched $zno_{1-x}te_x$ alloys," *Appl. Phys. Lett.* **106**, 092101 (2015).

[5] M.Saito and S.Fujihara, "Large photocurrenr generation in dye-sensitized zno solar cells," *Energ. Environ. Sci.* **1**, 280 (2008).

[6] B.Hussain, A.Ebong, and I.Ferguson, "Zinc oxide as an active n-layer and antireflection coating for silicon based solar cell," *Sol. Energ. Mat. Sol. Cells* **139**, 95 (2015).

[7] S.J.Young, L.W.Ji, T.H.Fang, S.J.Chang, Y.K.Su, and X.L.Du, "Zno ultraviolet photodiodes with pd contact electrodes," *Acta Meaterialia* **55**, 329 (2007).

[8] S.J.Jia, Zhang, Z. Z., Lu, Y. M., Shen, D. Z., Yao, B., Zhang, J. Y., Li, B. H., Zhao, D. X., Fan, X. W., and Tang, Z. K., "Zno p-n junction light-emitting diodes fabricated on sapphire substrates," *Appl. Phys. Lett.* **88**, 031911 (2006).

[9] P.S.Vachhani, ipr, O., Bhatnagar, A., Ramamoorthy, R., Choudhary, R., Phase, D., Dalba, G., Kuzmin, A., and Rocca., F., "Local structure and magnetization of ferromagnetic cu-doped zno films: No magnetism at the dopant?," *J. Alloys Compd.* **678**, 304 (2016).

[10] Barasheed, A., Kumar, S., and Alshareef, H., "Temperature dependent thermoelectric properties of chemically derived gallium zinc oxide thin films," *J. Materials Chemistry C* **1**, 4122 (2013).

[11] Mele, P., Saini, S., Honda, H., Matsumoto, K., Miyazaki, K., Hagino, H., and Ichinose, A., "Effect of substrate on thermoelectric properties of al-doped zno thin films," *Appl. Phys. Lett.* **102**, 253903 (2013).

[12] Qu, X., Wang, W., Lv, S., and Jia, D., "Thermoelectric properties and electronic structure of al-doped zno," *Solid State Communications* **151**, 332 (2011).

[13] Tsubota, T., Ohtaki, M., Eguchi, K., and Arai, H., "Thermoelectric properties of al-doped zno as a promising oxidematerial for high-temperature thermoelectric conversion," *J. Materials Chemistry* **7**, 85 (1997).

[14] Ohtaki, M., Araki, K., and Yamamoto, K., "High thermoelectric performance of dually doped zno ceramics," *J. Electronic Materials* **38**, 1234 (2009).

[15] Jood, P., Mehta, R., Zhang, Y., Peleckis, G., Wang, X., Siegel, R., Borca-Tasciuc, T., Dou, S., and Ramanath, G., "Al-doped zinc oxide nanocomposites with enhanced thermoelectric properties," *Nano letters* **11**, 4337 (2011).

[16] W.T.Chang, Y.C.Chen, R.C.Lin, C.C.Cheng, K.S.Kao, and Y.C.Huang, "Wind-power generators based on zno piezoelectric thin films on stainless steel substrates," *Curr. Appl. Phys.* **11**, S333 (2011).

[17] J.Song, J.Zhou, and Z.L.Wang, "Piezoelectric and semiconducting coupled power generating process of a single zno belt/wire. a technology for harvesting electricity from the environment," *Nano Lett.* **6**, 1656 (2006).

[18] Z.L.Wang and J.Song, "Piezoelectric nanogenerators based on zinc oxide nanowire arrays," *Science* **312**, 242 (2006).

[19] M.Y.Choi, D.Choi, M.J.Jin, I.Kim, S.H.Kim, J.Y.Choi, S.Y.Lee, J.M.Kim, and S.W.Kim, "Mechanically powered transparent flexible charge-generating nanodevices with piezoelectric zno nanorods," *Adv. Mater.* **21**, 2185 (2009).

[20] M.Lee, C.Y.Chen, S.Wang, S.N.Cha, Y.J.Park, J.M.Kim, L.J.Chou, and Z.L.Wang, "A hybrid piezoelectric structure for wearable nanogenerators," *Adv. Mater.* **24**, 1759 (2012).

[21] Pandey, A., Tyagi, V., Selvaraj, J. A., Rahim, N., and Tyagi, S., "Recent advances in solar photovoltaic systems for emerging trends and advanced applications," *Renew. Sust. Energ. Rev.* **53**, 859 (2016).

[22] Khan, J. and Arsalan, M. H., "Solar power technologies for sustainable electricity generation - a review," *Renew. Sust. Energ. Rev.* **55**, 414 (2016).

[23] Razykov, T. M., Ferekides, C., Morel, D., Stefanakos, E., Ullal, H. S., and Upadhyaya, H. M., "Solar photovoltaic electricity: Current status and future prospects," *Solar Energy* **85**, 1580 (2011).

[24] Young, S., Ji, L., Chang, S., and Su, Y., "Zno metalsemiconductormetal ultraviolet sensors with various contact electrodes," *J. Crystal Growth* **293**, 43 (2006).

[25] Liang, S., Sheng, H., Liu, Y., Huo, Z., Lu, Y., and Shen, H., "Zno schottky ultraviolet photodetectors," *J.Crystal Growth* **225**, 110 (2001).

[26] Li, Y., Li, X., and Gao, X., "Effects of post-annealing on schottky contacts of pt/zno films toward uv photodetector," *J. Alloys and Compounds* **509**, 7193 (2011).

[27] Basaka, D., Amin, G., Mallik, B., Paul, G., and Sen, S., "Photoconductive uvdetectors on solgel-synthesized zno films," *J.Crystal Growth* **256**, 73 (2003).

[28] Lin, T., Chang, S., Su, Y., Huang, B., Fujita, M., and Horikoshi, Y., "Zno msm photodetectors with ru contact electrodes," *J.Crystal Growth* **281**, 513 (2005).

[29] Chen, Z. H., Tang, Y. B., Liu, C., Leung, Y., Yuan, G., L.M. Chen and, Y. W., Bello, I., Zapien, J. A., Zhang, W. J., Lee, C. S., and Lee, S. T., "Vertically aligned zno nanorod arrays sentisized with gold nanoparticles for schottky barrier photovoltaic cells," *J. Phys. Chem. C* **113**, 13433 (2009).

[30] Bora, T., Kyaw, H., Sarkar, S., Pal, S., and Dutta, J., "Highly efficient zno/au schottky barrier dye-sensitized solar cells: Role of gold nanoparticles on the charge-transfer process," *Beilstein J. Nanotechnol.* **2**, 681 (2011).

[31] Hamad, O., Braunstein, G., Patil, H., and Dhere, N., "Effect of thermal treatment in oxygen, nitrogen, and air atmospheres on the electrical transport properties of zinc oxide thin films," *Thin Solid Films* **489**, 303 (2005).

[32] Ruske, F., Roczen, M., Lee, K., Wimmer, M., Gall, S., Hupkes, J., Hrunski, D., , and Rech, B., "Improved electrical transport in al-doped zinc oxide by thermal treatment," *J. Appl. Phys.* **107**, 013708 (2010).

[33] Yang, W., Wu, Z., Liu, Z., Pang, A., Tu, Y., and Feng, Z., "Room temperature deposition of al-doped zno films on quartz substrates by radio-frequency magnetron sputtering and effects of thermal annealing," *Thin Solid Films* **519**, 31 (2010).

[34] Braga, A., Moreira, S., Zampieri, P., Bacchin, J., and Mei, P., "New processes for the production of solar-grade polycrystalline silicon: A review," *Solar Energy Materials & Solar Cells* **92**, 418 (2008).

[35] Ip, K., Thaler, G., Yang, H., Han, S. Y., Li, Y., Norton, D., Pearton, S., Jang, S., and Ren, F., "Contacts to zno," *J. Crystal Growth* **287**, 149 (2006).

[36] Polyakov, A. Y., Smirnov, N. B., Kozhukhova, E. A., Vdovin, V. I., Ip, K., Heo, Y. W., Norton, D. P., and Pearton, S. J., "Electrical characteristics of au and ag schottky contacts on n-zno," *Appl. Phys. Lett.* **83**, 1575 (2003).

[37] Ajimsh, R., Vanaja, K., Jayaraj, M., Misra, P., Dixit, V., and Kukrej, L., "Transparent p-agcoo$_2$/n-zno diode heterojunction fabricated by pulsed laser deposition," *Thin Solid Films* **515**, 7352 (2007).

[38] Arcari, M., Scarpa, G., Lugli, P., Member, S., Tallarida, G., Huby, N., Guziewicz, E., Krajewski, T. A., and Godlewski, M., "2-d finite-element modeling of zno schottky diodes with large ideality factors," *IEEE Trans. on Elect. Dev.* **59**, 2762 (2012).

[39] Lu, N. and Ferguson, I., "Iii-nitrides for energy production: photovoltaic and thermoelectric applications," *Semiconductor Science and Technology* **28**, 074023 (2013).

[40] Tritt, T. and Subramanian, M., "Thermoelectric materials, phenomena, and applications: a bird's eye view," *MRS bulletin* **31**, 188 (2006).

[41] Wang, B., Kucukgok, B., He, Q., Melton, A., Leach, J., Udwary, K., Evans, K., Lu, N., and Ferguson, I., "Thermoelectric properties of undoped and si-doped bulk gan," *MRS Online Proceedings Library Archive* **1558**, 1 (2013).

[42] Jood, P., Mehta, R., Zhang, Y., Borca-Tasciuc, T., Dou, S., Singh, D., and Ramanath, G., "Heavy element doping for enhancing thermoelectric properties of nanostructured zinc oxide," *RSC Advances* **4**, 6363 (2014).

[43] Dalafave, D., "Thermoelectric properties of $\mathrm{re}_6\mathrm{ga}_x\mathrm{se}_y\mathrm{te}_{15-y}$," *Materials Chemistry and Physics* **119**, 195 (2010).

[44] Yigen, S. and Champagne, A., "Wiedemann-franz relation and thermal-transistor effect in suspended graphene," *Nano letters* **14**, 289 (2013).

[45] Kucukgok, B., Hussain, B., Zhou, C., Ferguson, I., and Lu, N., "Thermoelectric properties of zno thin films grown by metal-organic chemical vapor deposition," *MRS Proceedings* **1805**, mrss15–2136936 (2015).

[46] Brockway, L., Vasiraju, V., Sunkara, M., and Vaddiraju, S., "Engineering efficient thermoelectrics from large-scale assemblies of doped zno nanowires: Nanoscale effects and resonant-level scattering," *ACS applied materials & interfaces* **6**, 14923 (2014).

[47] Balandin, A., "Thermal properties of graphene and nanostructured carbon materials," *Nature materials* **10**, 569 (2011).

[48] Ohtaki, M., Tokunaga, T., Eguchi, K., and Arai, H., "August. hopping carrier mobilities and thermoelectric properties of oxide materials with perovskite-related structure," *Proceedings ICT'97. XVI International Conference on IEEE* , 224 (1997).

[49] Saini, S., Mele, P., Honda, H., Henry, D., Hopkins, P., Molina-Luna, L., Matsumoto, K., Miyazaki, K., and Ichinose, A., "Enhanced thermoelectric performance of al-doped zno thin films on amorphous substrate," *Japanese J. Appl. Phys.* **53**, 060306 (2014).

[50] Martin, J., "Apparatus for the high temperature measurement of the seebeck coefficient in thermoelectric materials," *Review of Scientific Instruments* **83**, 065101 (2012).